

PAPER • OPEN ACCESS

Relationship between magnetic field and tokamak size—a system engineering perspective and implications to fusion development

To cite this article: G. Federici *et al* 2024 *Nucl. Fusion* **64** 036025

View the [article online](#) for updates and enhancements.

You may also like

- [Electromagnetic-mechanical coupling analysis of high-temperature superconducting racetrack coil](#)
Liuyuan Yu, Mengdie Niu, Huadong Yong et al.
- [First performance test of a 25 T cryogen-free superconducting magnet](#)
Satoshi Awaji, Kazuo Watanabe, Hidetoshi Oguro et al.
- [A new method for avoiding critical current degradation of YBCO coils using ice impregnation](#)
Guangda Wang, Hangwei Ding, Rui He et al.

Relationship between magnetic field and tokamak size—a system engineering perspective and implications to fusion development

G. Federici^{1,2,*}, M. Siccino^{1,3}, C. Bachmann¹, L. Giannini¹, C. Luongo¹
and M. Lungaroni⁴ 

¹ Consortium EUROfusion, Boltzmannstr. 2, 85748 Garching, Germany

² On assignment from Fusion for Energy, Josep Pla, No. 2 Torres Diagonal Litoral, 08019 Barcelona, Spain

³ On assignment from Max Planck Institut für Plasmaphysik, Boltzmannstr. 2, 85748 Garching, Germany

⁴ Department of Industrial Engineering, University of Rome ‘Tor Vergata’, Via del Politecnico 1, 00133 Rome, Italy

E-mail: gianfranco.federici@euro-fusion.org

Received 4 August 2023, revised 4 January 2024

Accepted for publication 30 January 2024

Published 14 February 2024



CrossMark

Abstract

High temperature superconductors (HTSs) offer the promise of operating at higher magnetic field and temperature. Recently, the use of high field magnets (by adopting HTS) has been promoted by several groups around the world, including new start-up entries, both to substantially reduce the size of a fusion power reactor system and as a breakthrough innovation that could dramatically accelerate fusion power deployment. This paper describes the results of an assessment to understand the impact of using high field magnets in the design of DEMO in Europe, considering a comprehensive list of physics and engineering limitations together with the interdependencies with other important parameters. Based on the results, it is concluded that increasing the magnetic field does not lead to a reduction in device size with relevant nuclear performance requirements, because (i) large structures are needed to withstand the enormous electromagnetic forces, (ii) thick blanket and n-shield structures are needed to protect the coils from radiation damage effects, and (iii) new divertor solutions with performances well beyond today's concepts are needed. Stronger structural materials allow for more compact tokamaks, but do not change the conclusion that scalability is not favourable when increasing the magnetic field, beyond a certain point, the machine size cannot be further reduced. More advanced structural support concepts for high-field coils have been explored and concluded that these solutions are either unfeasible or provide only marginal size reduction, by far not sufficient to account for the potential of operating at very high field provided by HTS. Additionally,

* Author to whom any correspondence should be addressed.



Original content from this work may be used under the terms of the [Creative Commons Attribution 4.0 licence](https://creativecommons.org/licenses/by/4.0/). Any further distribution of this work must maintain attribution to the author(s) and the title of the work, journal citation and DOI.

the cost of high field coils is significant at today's price levels and shows to scale roughly with the square of the field. Nevertheless, it is believed that even when not operated at high field and starting within conventional insulated coils, HTS can still offer certain benefits. These include the simplification of the magnet cooling scheme thanks to increased temperature margin (indirect conduction cooling). This in turn can greatly simplify coil construction and minimize high-voltage risks at the terminals.

Keywords: high temperature superconductors, magnetic field, DEMO, magnets

1. Introduction

The relationship between magnetic field on the plasma and its performance metrics are well known. The discovery of and recent developments on high temperature superconductors (HTSs) have created the expectation that fusion devices could operate at much higher magnetic fields than previously foreseen, and thus may offer the breakthrough needed to make fusion energy a reality. A parametric system study is presented in this paper that explores the trade-off between benefits and constraints when designing tokamaks at increasingly higher magnetic fields. The aim of the study is to quantify potential benefits, but also to highlight how other technology or practical considerations affect the scaling of tokamak size with increasing magnetic field.

In this work, the focus was on tokamak machines based on deuterium–tritium (D–T) fusion reactions, which is the most commonly selected reaction by virtue of its high cross section at plasma temperatures of the order of 10–20 keV. Recently, alternative fusion reactions, such as $D + He^3$, which avoid both the use of T and the production of 14 MeV neutrons, have gained renewed interest. A tokamak power plant based on such reactions will unavoidably require a very high magnetic field for operation. This is due to the extremely high temperatures (and/or densities) at which the plasma must be operated to attain a sufficient reaction cross section. Consequently, plasma pressure increases which has to be counteracted by enhancing the magnetic field to avoid plasma instabilities (e.g. the so-called beta limit). In this sense thus, the analysis of high field devices also applies to concepts employing alternative reactions to D–T—providing a tokamak concept is envisaged.

The basic geometrical expressions that determine tokamak size and radial build for a generic fusion device based on the standard structural concept of wedged toroidal field (TF) coils are first introduced. The study is then presented, consisting of assessing tokamak size versus magnetic field, while keeping the fusion power constant. The two main constraints that prevent continuous size reduction as magnetic field is increased are subsequently discussed. These technical limits are the increase in structural demands, as well as increase in the heat load on the divertor (power exhaust). The next section presents how the tokamak size scales with magnetic field when these technical constraints are introduced, and how they prevent size

reductions beyond a certain point as magnetic field continues to increase. Beyond geometrical, structural, or power exhaust constraints, the paper then discusses other aspects that also tend to limit size reductions when field is increased, namely, the cost associated and the manufacturability constraints as the TF coil structures grow in size towards practical limits. A relative quantification of how cost scales with increasing field shows that as field increases in an attempt to reduce size, TF coil cost actually increases significantly.

Even though the conclusion of the study indicates there are limits to effectively increase the magnetic field in power plant-relevant fusion reactors, the benefits promised by HTS materials are recognized. The paper concludes with a proposal for a HTS development and qualification program specifically targeting those aspects with the greatest benefit to fusion power plant design, such as DEMO.

2. Background

2.1. Tokamak basic geometrical considerations

The power density in a tokamak is given by:

$$P_F \propto \beta_t^4 B_{T,o}^4 \quad (1)$$

where β_t (*beta*) is the plasma kinetic-to-magnetic pressure ratio and $B_{T,o}$ is the TF strength at the centre of the plasma. By increasing $B_{T,o}$ and/or *beta* one clearly obtains a significant increase in power density. However, *beta* is limited by plasma stability and $B_{T,o}$ is limited by the achievable peak field, $B_{T,m}$, at the magnet windings, in turn limited by superconducting material capabilities. Depending on the required magnet peak field, the superconductor of choice must transition from NbTi, to Nb₃Sn, to Rare-Earth Barium Copper Oxide (REBCO), with the consequent step-changes in manufacturing approach, technology maturity level, and cost depending on design approach.

A critical design feature of any tokamak is the space taken up by the inner leg of the TF coil (Δ_{TF} see figure 1). The radial build needed for the TF coil inner leg, along with the size of the central solenoid (CS), the size of the vessel/n-shielding/T-breeding regions and the plasma minor radius determine the major radius of the machine.

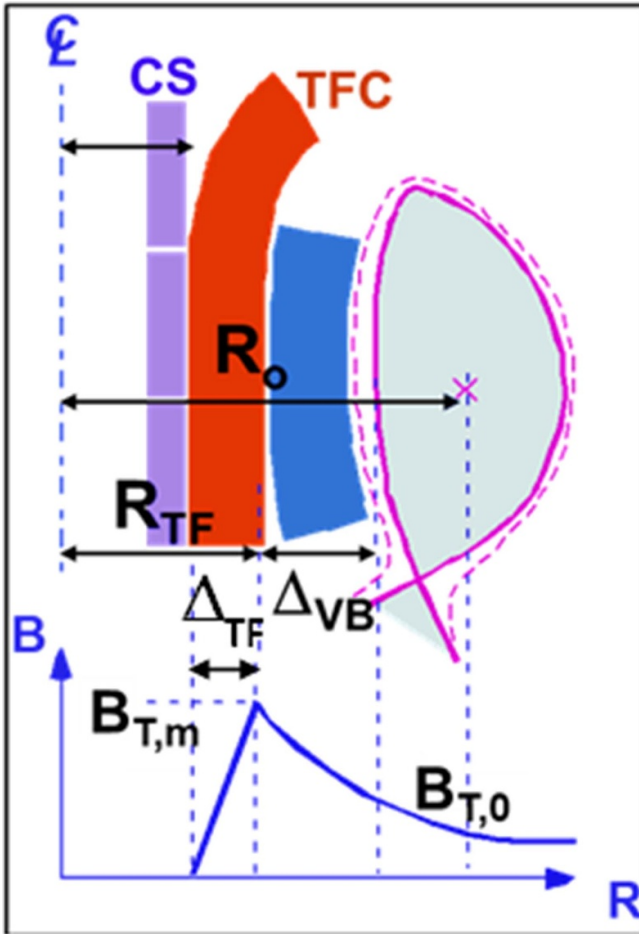


Figure 1. Simplified radial build of a tokamak showing the key fusion components at the inboard: CS, TF coils, Shield and Breeding blanket.

The relationship between $B_{T,m}$ and $B_{T,o}$ is given by (see figure 1):

$$B_{T,o} \cong \frac{(A-1)}{A} \left(1 - \frac{\Delta_{VB} A}{R_0 (A-1)} \right) B_{T,m} \quad (2)$$

where A is the aspect ratio (R/a) (for ITER $A = 3.1$), R_0 is the major radius of the plasma, and Δ_{VB} is the thickness of the region occupied at the inboard by the breeding blanket and the vacuum vessel including the space required to assemble the thermal shield (i.e. the distance in mid-plane from the first wall to the TF coil windings).

In contrast to devices with a pure burning plasma physics mission and very limited neutron fluence (i.e. SPARC), power-plant demonstration devices with extensive nuclear performance ambitions require very thick shield/blanket structures to protect the magnets and the vacuum vessel from radiation heating and damage effects and for tritium breeding. This increases the maximum value of the magnetic field in the inner TF coil leg $B_{T,m}$, for a given magnetic field value in the centre of the plasma $B_{T,o}$ (figure 1).

It should be noted that higher field windings generate higher forces in the mechanical structures in and around the plasma

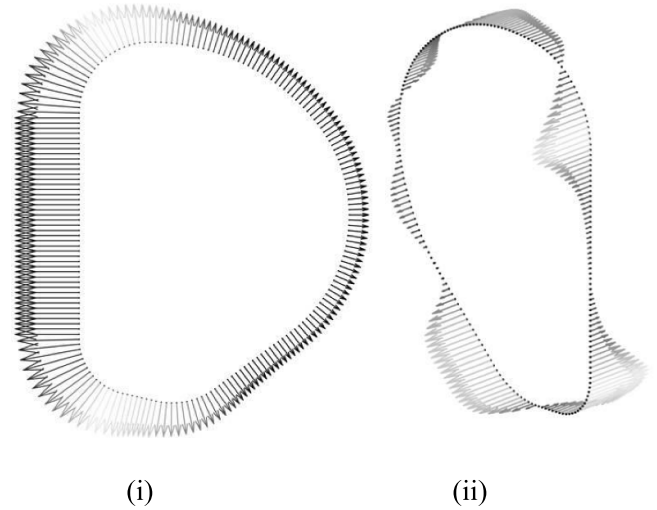


Figure 2. Schematic of (i) in-plane and (ii) out-of-plane loads on a TF coil.

and in particular in the TF coils themselves, which constitutes the structural core of the machine. The stresses in the inboard leg of the TF coil casing quickly reach the maximum allowable stress for a given geometry, effectively limiting the field. This stress roughly scales with B^2/S (where S is cross section of the structural elements).

2.2. TF coil structural considerations

The cross section of the TF coil inner leg must support in-plane forces i.e. the centring force and that portion of the vertical separating force that is not supported by the outer structures. In this study, the TF coil inner leg equatorial plane cross sections are considered. Out-of-plane (OOP) forces that result from the interaction between the TF coil currents and the poloidal field must also be supported within the TF coil system. The OOP forces are mostly absorbed by structures that are not closely coupled with the radial build of the central column and they are not discussed here.

Figure 2 schematically shows the typical loads on a tokamak TF coil. The TF strength and thus the local magnetic pressure is proportional to $1/r$ inside the bore of the TF coils. Magnetic pressures at the top and bottom of the coil integrate to vertical separating forces. The inner leg magnetic pressure integrates to a centring force on the inner leg.

The approximate calculation of these forces follows [1]:

$$F_{\text{vert}} = \frac{1}{4} B_{T,o} R_0 I_{TF} \ln \frac{R_{\text{outb}}}{R_{\text{inb}}} \quad (3)$$

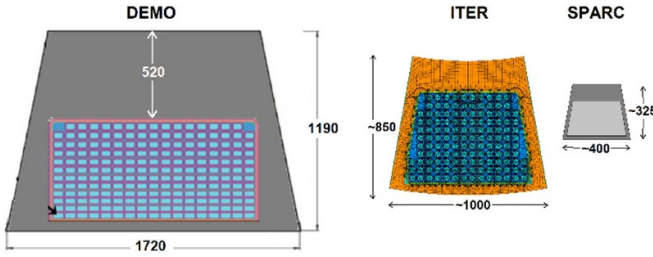
$$\frac{F_{\text{rad}}}{m} = \frac{1}{2} I_{TF} B_{T,m} \quad (4)$$

where I_{TF} is the total Amp-turns in the TF coils, R_{outb} and R_{inb} are the radii of the TF coil leg of the outboard and inboard, respectively.

Table 1 shows key parameters and the resulting vertical and centring forces on the inner leg of the TF coils for ITER [2, 3] and SPARC [4, 5] (both under construction), and those

Table 1. Main machine parameter comparison.

	DEMO	ITER	SPARC
I_{TF} (total Amp-turns) (MA)	14.9	8.4	6.5
$B_{t,m}$ (T)	13	10.8	21.7
R_{TF} inb. leg (m)	4.3	2.7	~ 1
$A_{inb,leg}$ (WP) (m ²)	0.69	0.48	~ 0.05
J_{WP} (A mm ⁻²)	21	17.5	120
F_{vert} (MN)	275	100	50
$\frac{F_{rad}}{m}$ (MN)	90	50	70

**Figure 3.** Mid-plane cross-section of the TF coil of DEMO, ITER, and SPARC.

predicted for the European DEMO [6]. Figure 3 shows the mid-plane cross-section of the TF coil of ITER, DEMO and SPARC.

One can observe that the electromagnetic forces related to ITER and SPARC are of the same order of magnitude despite the latter being a much smaller machine.

Robust structural concepts are needed to enable the set of TF coils (18 in ITER) to withstand the centring and vertical forces. Several concepts have been investigated in the past including full wedging, or partial wedging, and bucking against a CS or bucking post. A review of these concepts, plus some new ideas, were analysed in the context of DEMO-like machines [7]. However, all concepts relying on bucking are very complicated in practice, as they require the TF coil to slide against the bucking cylinder or the CS coil to accommodate motion during operation. Very complex structural designs are needed to support OOP loads on the TF coils without transferring this twist to the CS. For the bucked and wedged configuration, detailed analyses show that the stress on the TF leg is extremely sensitive to the assembly tolerance between TF coils and CS (or whatever bearing surface is placed in-between). Sub-millimetre tolerances are to be achieved over the large contact surface for the stress distribution to be predictable, which is impractical. After in-depth assessments conducted during the design phase, ITER opted for full wedging of the TF coils.

To minimise the fraction of vertical force to be reacted by the inner legs, various options have been investigated including TF coil pre-compressive preloads, sliding joints and heavy external structures that compromise the access for maintainability and increase the cost. These were explored together with alternative structural support concepts [7] and it was concluded that, for DEMO-size machines, most of the potential solutions are either not feasible or provide only marginal structural reduction given their complexity. Scalability of alternate

structural concepts was not evaluated, the remaining of this study focuses on the wedged TF coil concept, as implemented in ITER.

2.3. Interdependency with the power exhaust

By varying the size of the device and the magnetic field strength, the power exhaust conditions of the device can change significantly. In this section, the link of the heat flux on the divertor with the machine R_0 and $B_{T,o}$ is briefly illustrated. According to the broadly employed Eich scaling [8, 9], the heat load channel width in the scrape-off-layer λ_q scales unfavourably with the field strength but only very weakly with the major radius,

$$\lambda_q = 0.73 B_{T,0}^{-0.78} q_{95}^{1.2} R_0^{0.1}. \quad (5)$$

This reflects the fact that a high magnetic field and compact machine possesses a higher energy density than low field devices. In the formula, q_{95} is the so-called edge safety factor at the 95% magnetic flux surface and is roughly proportional to the ratio between the toroidal field strength in the plasma and the plasma current. To determine the power crossing the plasma separatrix, the assumption has been made that the power crossing the separatrix for the design points considered is proportional to the power to the L- to H-mode transition, P_{LH} , following the widely employed Martin scaling [10]

$$P_{LH} = 0.049 n^{0.72} B_{T,0}^{0.8} S_p^{0.94} \quad (6)$$

where S_p is the plasma surface and the density n has in turn been assumed proportional to the Greenwald density limit

$$n \propto n_{GW} = \frac{I_p}{\pi a^2} \quad (7)$$

where I_p is the plasma current, a is the minor plasma radius.

In order to sustain H-mode, the power crossing the separatrix P_{sep} , and thus the plasma heating power, shall not drop below this threshold power. On the other hand, it is desirable to keep P_{sep} as low as possible for divertor protection. In all EU-DEMO configurations, the heating power (both from fusion reactions and auxiliary heating) largely exceeds the value of P_{LH} by a factor of 3–4. Therefore, in order to protect the divertor by facilitating the achievement of detachment, and in general to reduce the heat flux in case of accidental attachment conditions, the ability to reliably radiate a large fraction (75%–80%) of the heating power from the plasma core by means of seeded impurity (Xe or Kr), until the condition $P_{sep} = f_{LH} P_{LH}$ is met with $f_{LH} = 1.1 - 1.2$ for controllability reason [11].

The heat flux on the divertor under attachment conditions (q_{tar}) is then proportional to the power crossing the separatrix divided by the wetted area, which in turns depend on λ_q :

$$q_{tar} \propto \frac{P_{sep}}{2\pi R_0 \lambda_q}. \quad (8)$$

Employing the Eich scaling and the Martin scaling, and assuming constant plasma shape (q_{95} , elongation and triangularity), it can be easily shown that:

$$q_{tar} \propto f_{LH} B_{T,0}^{2.52} R_0^{0.16} \quad (9)$$

Reference [12] provides the full and detailed calculation. This last relation indicates that generally speaking, a compact high-field device is expected to be more challenging in terms of power exhaust. Clearly, no fusion power reactor is expected to operate under attached divertor condition, because the fluxes will be almost certainly too high. Thus, some kind of dissipation for the achievement of detachment must be introduced. Still, it is thought that the divertor heat flux under attachment is a representative figure of merit to compare different design solutions. A reactor must work with long pulse, and the possibility of losing divertor detachment has to be considered from the earliest design phases. Comparing q_{tar} under attached divertor conditions therefore provides a good indication about how challenging the power exhaust problem is, at least in relative terms.

Both this quick overview and the more detailed calculation in [12] assume a plasma in H-mode. This assumption is motivated by the fact that H-mode exhibits the highest plasma confinement (and thus the maximum fusion power generation in reactors) for a given machine architecture. Thus, such a regime is the most obvious choice to minimise the machine size. Most alternative regimes also show a minimum threshold power to be accessed, and while the dependency of the threshold on the magnetic field strength can vary (e.g. the I-mode [13] threshold power P_{LI} has been shown to have a weaker dependency on the field, i.e. $P_{LI} \sim B_{T,0}^{0.26}$ [14]), an increase of the threshold power with increasing field is always observed. For this reason, the argument presented here remains valid, at least from a qualitative point of view—namely, there will always be a field strength above which the divertor protection constraints prevent further size reduction at constant fusion power.

This is no longer valid if the chosen plasma operating regime does not need a minimum threshold power to be sustained. This is the case, for example, for the negative triangularity L-mode [15, 16], which however, in spite of the very significant advances in the last years, still remains quite speculative.

For these regimes, only the radial build holds limiting factor for decreasing the size, as explained below in detail. In the following, only H-mode will be anyway considered.

3. Effect of magnetic field on machine size

In this section an exploration of machine size versus magnetic field is presented. To size the TF coils, winding pack designs are based on the assumption of insulated cable-in-conduit conductor (CICC), even for HTS coils. Although other concepts such as non-insulated (NI) coils may offer higher current densities, they were not considered here as they are still developmental and unproven on the scale of electricity-producing fusion machines. For the structures, ITER materials are used in the sizing. One of the lessons from ITER is that developing stronger structural materials is a decades-long effort, without assurance of success [17]. The effect on scaling of using stronger materials for the TF coil structures is discussed as part of parametric explorations in section 4 (see 4.3).

The aim is to quantify how machine size scales with magnetic field. To that end, PLASMOD, a simplified plasma transport code based on ASTRA [18] is used to determine the dimensions of the plasma. PLASMOD solves the 1D steady-state plasma transport equations (continuity and energy for all species) in the approximation of Bohm-gyroBohm transport coefficients. The seeded impurity concentration in the plasma core is changed until the power crossing the separatrix reaches the target value imposed by the user (typically close to the $L-H$ threshold). This code has the advantage of being reasonably fast (around ~ 10 s for each point) while avoiding an imposed shape for the plasma profiles, as most simplified transport codes do. PLASMOD calculates the plasma kinetic profiles—and hence all the related scalar quantities like e.g. the fusion power and the plasma β —employing plasma geometry (R_0 , $B_{T,0}$, elongation and triangularity) and edge safety factor q_{95} , among others, as input.

Figure 4 shows the results of the exploration with the major radius (R_0) plotted as a function of the field at the centre of the plasma ($B_{T,0}$) for the European DEMO device (~ 2000 MW of fusion power) for three cases as described below. All the machines in figure 4 have an aspect ratio $A = 3.1$. The three curves displayed in figure 4(i) have been obtained as follows:

- (a) This case accounts *only* for physics consideration and ignores any geometrical and/or engineering constraints: the magnetic field $B_{T,0}$ is employed as scan parameter and, for each $B_{T,0}$, the major radius is varied until the target $P_{\text{fus}} = 2000$ MW is achieved. No engineering constraint is taken into account in this case. Aspect ratio A and edge safety factor q_{95} have been kept constant for all points ($A = 3.1$ and $q_{95} = 3.5$, respectively). This is the smallest theoretical machine producing the given power.
- (b) In this case, the constraint arising from the need to protect the divertor from excessive heat loads is considered (see section 2.3). This curve is calculated following the same logic as the previous one, with the difference that the constraining criterion is not related to the radial build, but to the divertor figure of merit:

$$\frac{P_{\text{sep}}B}{qAR} < 9.2 \text{ MW T/m} \quad (10)$$

where P_{sep} has been set to $1.1P_{LH}$, assuming that the remaining heating power is exhausted in form of electromagnetic radiation from seeded impurity, as typically assumed for the European DEMO [11]. The value of P_{LH} is in turn provided by PLASMOD. The value of 9.2 MW T m^{-1} roughly corresponds to a heat flux on the divertor of $\sim 70 \text{ MW m}^{-2}$ by reattachment and can be shown to be the ITER baseline value [12]. As for the previous case, the value of q_{95} is progressively increased until a solution at $P_{\text{fus}} = 2000$ MW is found, which fulfils the constraining criterion. This ensures a minimisation of the size.

- (c) In this case, the most complex geometrical radial build constraints at the inner leg (see figure 1) arising from the

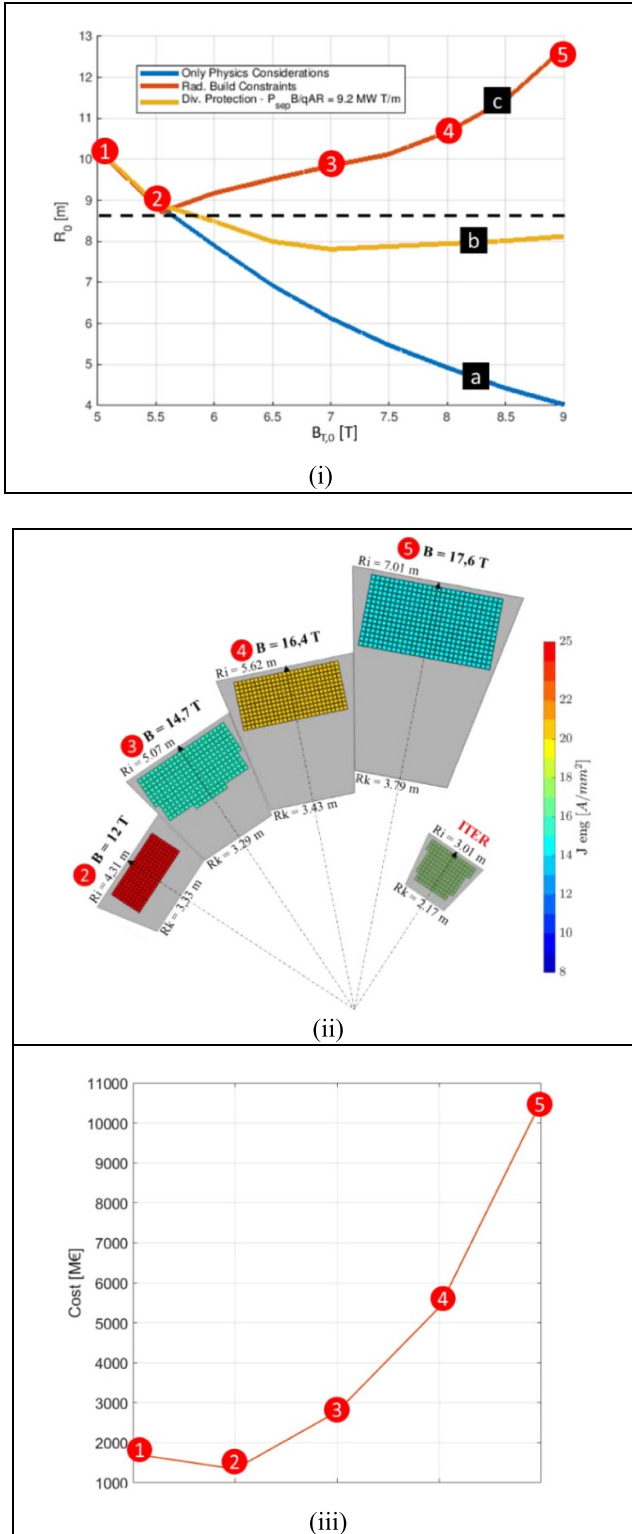


Figure 4. (i) Effect of plasma axis magnetic field ($B_{T,0}$) on machine size (R_0) at constant fusion power (2GW) and constant aspect ratio ($A = 3.1$); (ii) cross-section and current density of the TF coils, (iii) estimated cost of TF coils.

CS and TF coil winding pack/structure sizing to withstand the forces are introduced. Once the radius providing $P_{fus} = 2000$ MW is found, a check on the radial build

consistency is carried out. The detailed steps to undertake this were:

- The size of the external radius of the CS (R_{CS} in figure 1) is calculated by means of look-up tables, which have been generated following the methodology developed and described in [19]. These tables provide the external radius of the CS for a fixed value of the vertical field as a function of the pre-magnetisation flux and of the number of plasma cycles n_{cyc} , to account for the role of the fatigue in the dimensioning of the component. While the latter value has been set constant to $n_{cyc} = 30.000$, the former is determined as a function of the plasma loop voltage V_{loop} (calculated with PLASMOD) and of the plasma internal inductance. In the present work, only a pulsed device is referred to, which possesses a CS to sustain the plasma current for a burn time of 2 h (except where otherwise stated). Clearly, the CS has a significant impact on the overall size of the device. However, the main point illustrated in figure 4—i.e. that an increase in magnetic field cannot lead to a reduction of the machine size for a given performance because of the increase in the TF coil size to withstand the forces—is perfectly valid also for non-inductive, steady-state devices, where the CS is much smaller or even absent.
- The radial size of the TF coils (Δ_{TF} in figure 1) to withstand the forces generated by the field is determined via an integrated algorithm, which takes into account a specific plasma shape, position, and field. By adjusting various factors such as the operating current, number of layers and turns, maximum voltage, and materials used in the winding pack layout, different manufacturing options are explored, and maximum stress levels applied in the algorithm. The resulting outcome is a balanced solution that optimizes the engineering current density while minimizing the radial build while respecting quench protection and structural limits [20].
- The thickness of the breeding blanket, vacuum vessel and thermal shielding (Δ_{VB} in figure 1) has been kept constant for all points and set equal to 1.4 m as a result from previous work [21].

If the radial build is consistent—i.e. if there is enough space for the CS in the bore—the point is considered acceptable. If not, the analysis is repeated for a higher value of q_{95} , since for a given field B_0 , a larger machine must have a lower current to have the same fusion power $P_{fus} = 2000$ MW. This procedure ensures that the point found is the smallest possible machine fulfilling the given constraints.

Note that once engineering constraints are introduced (cases b and c), feasible machines are significantly larger than the theoretical minimum. Not only does increasing field lead to larger machines, but the associated needs for superconductors and structures also drive the cost significantly (see figure 4(iii)). Section 5 expands on the methodology to determine relative cost of the TF coils.

4. Parametric exploration of machine size

In the previous section, the exploration of the magnetic field as a variable assumed a constant aspect ratio for the machine (and for each point finding the minimum size). This section presents a parametric exploration showing the main conclusions are not altered if other parameters are varied as a minimum size machine is targeted. The effect of aspect ratio and fusion power variations on machine size are quantified in the following sub-sections.

4.1. Effect of aspect ratio

As part of the DEMO re-baselining, following the Gate G1, the benefit of adopting a lower value of the machine aspect ratio has been explored. This includes:

- A reduction of the field in the plasma, and hence in the TF coils, to achieve the same fusion power output, leading to appreciable advantages in terms of fabricability and costs.
- A reduction of the maximum heat flux at the divertor in case of reattachment. This of course reduces the risk of the machine operation, enhancing the control margins and, possibly, simplifying the whole design.
- An increase of the elongation, which leads to a larger fusion power for a given machine radius. This is due to both the higher natural elongation and to the fact that the passive structure is brought closer to the plasma, thus enhancing the passive stability of the equilibrium.

While figure 4 showed machine size versus magnetic field at constant aspect ratio, figure 5 shows that by increasing the machine aspect ratio, the field at the centre of the plasma increases and correspondingly the size of the plasma to sustain a given fusion power output (2 GW) is reduced substantially (see equation (1)). However, the machine major radius increases as a result of the increase of the TF coil radial build dimensions that increases with the field and the need to protect the divertor (see section 2.3). A low temperature superconductor (LTS) such as Nb_3Sn is the conductor used for peak field < 15 T, for cases TF1, TF2, and TF3 in figure 5, while case TF4 uses HTS. Note that case TF2 in figure 5 is the same as case 2 in figure 4 (same baseline).

4.2. Effect of varying the fusion power

To address the possible counter argument that the considerations described above on the need to have very massive TF coil structures is only linked to devices with high fusion power outputs (i.e. DEMO-class devices), the results of a study to compare two representative cases with very different values of fusion power and modes of operation are presented here.

Two cases were studied: one of a device producing 2000 MW of fusion power and operating in a pulsed mode with pulses of 2 h, and a second of a device producing 500 MW, operating in steady state (i.e. with a CS supposed to provide only the flux to ramp the current up to its nominal value, but not to sustain the flat-top). A high aspect ratio, $A=4$, has been

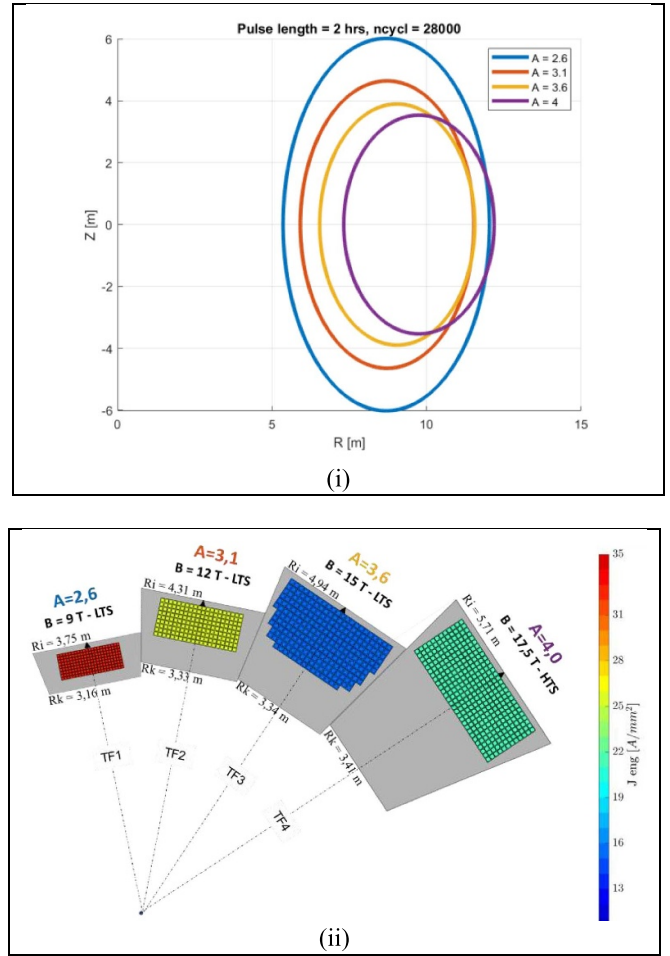


Figure 5. (i) Simplified plasma contours for a class of devices that produce a $P_{\text{fus}} = 2000$ MW, 2 h pulse and 3000 cycles at different aspect ratios. The values of the maximum field $B_{T,m}$ are (TF1): 9 T at $A = 2.6$, (TF2): 12 T at $A = 3.1$, (TF3): 15 T at $A = 3.6$, and (TF4): 17.5 T at $A = 4.5$, TF2 is the same machine as 2 shown in figure 4; (ii) mid-plane cross section of the TF coils (at 15 T or below conductor is LTS, above 15 T it is HTS, thus the discontinuity in current density).

chosen, to allow for solutions with high toroidal magnetic field ($B_{\text{max}} \sim 17.3$ T) — i.e. we concentrate our focus on the high field design points, without looking for the best possible configuration in a broad sense. This device with $P_{\text{fus}} = 500$ MW, similar to TF4 in figure 5 is referred to as TF4_R (reduced power). The results of this comparison are presented in figure 6 and show that even by reducing the fusion power by a factor of four, whilst maintaining the peak field, the radial thickness of the TF coils is not significantly reduced. It should be noted that the radial thickness of the shield/breeding blanket and vacuum vessel were assumed to be the same for both cases. As a matter of fact, the radial dimension of the breeding blanket is roughly independent of the device and the generated neutron flux intensity, as it must be defined primarily to ensure achieving the required tritium breeding capability (i.e. the probability of each neutron to interact with lithium and generate one Triton must be greater than 1, typically > 1.05). The thickness of the vacuum vessel and blanket shielding part are instead

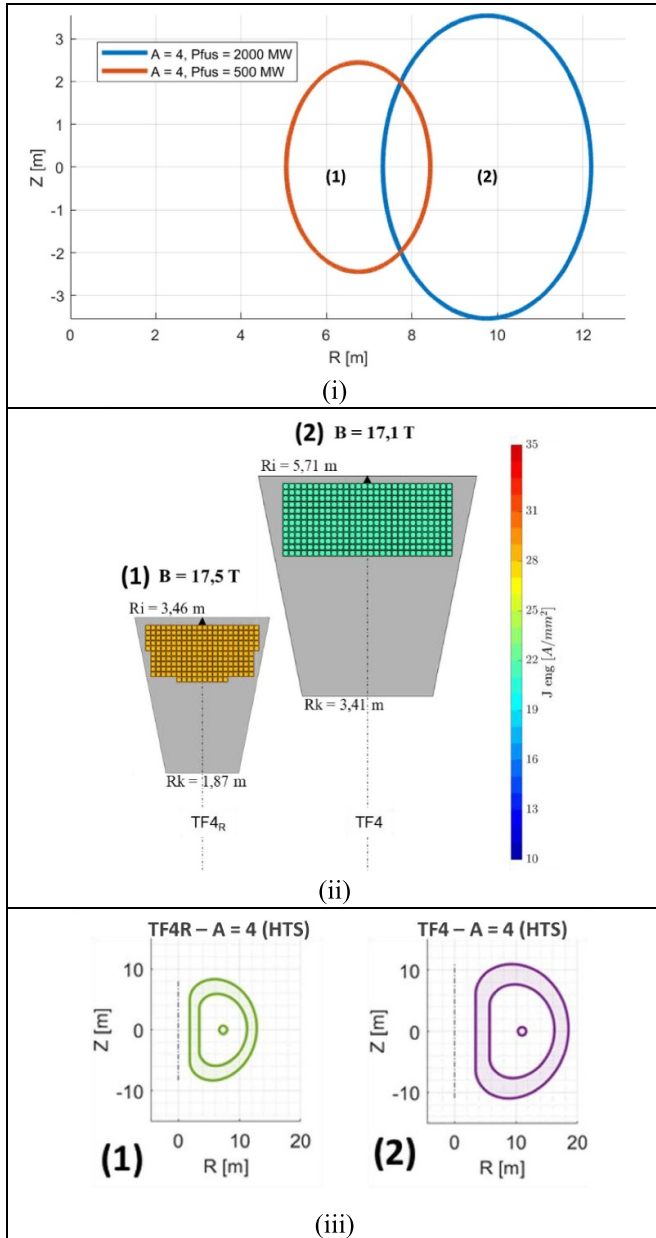


Figure 6. (i) Simplified plasma contours for two devices at $A = 4$: TF4, a pulsed (2 h) device with $P_{\text{fus}} = 2000$ MW, and TF4_R, a steady-state device with $P_{\text{fus}} = 500$ MW, (ii) mid-plane cross section of the TF coils; (iii) poloidal cross-section of the TF coils.

chosen to reduce the neutron flux by at least 5 orders of magnitude. Moderate variations of this flux e.g., by a factor of 2, do not significantly affect the required thickness [22]. It should also be noted that the major radius of case (1) in figure 6 (i) is mainly due to the fact that by assuming a steady-state plasma, the flux swing to be provided by the CS and, in turn, its radial build is much smaller than a pulsed plasma (see case (2) in figure 6). However, even with these assumptions the major radius cannot drop below 6-7 m (see figure 6) and, as will be detailed in section 5 (see figure 8), the cost of the TF coils remains comparable to that of larger machines with four times the power output, lower magnetic field and LTS coils.

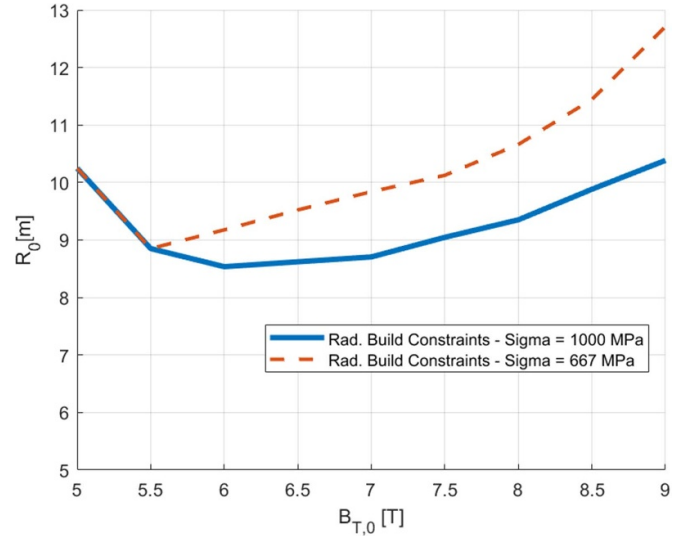


Figure 7. Variation of machine size with magnetic field when a structural material with 50% higher yield strength is used. The dashed curve is the same as the curve c) that is shown in figure 4(i).

4.3. Effect of improved structural materials

The parametric studies presented so far correspond to DEMO-like machines based on structural materials already developed and deployed in ITER. The question is whether by increasing the strength of the TF coil structure materials the machine could be made smaller and scalability with magnetic field is altered. To answer this, a scan of magnetic field was done as presented in figure 4 (same fusion power and aspect ratio), but now assuming the structures are made with a material with 50% higher yield strength at 4 K (i.e. 1500 MPa) than what has been proven at ITER-scale. The chosen value is slightly higher than what can be achieved with N50, a well-established material, although forgings of the size and thickness required for the TF coil nose may not be feasible. This caveat notwithstanding, the exercise is illustrative, as shown in figure 7. Employing a much stronger structural material allows for smaller machines, as expected. The optimum (minimum size) occurs at slightly higher magnetic field, also to be expected, but the overall trend remains: as magnetic field increases, the machine cannot become smaller due to the space requirements driven by space for the CS and TF coil nose (radial build). Therefore, the premise of making more compact tokamaks via new and stronger structural materials does not hold. Further, the development and qualification of these new materials and the fabrication routes to use them at the scale required in a fusion machine are not trivial, as discussed later in the paper, see section 6.

5. Dependence of TF coil costs on magnetic field

When exploring optimized machine configurations, it is important to consider not only all the technical requirements and constraints, but also costs. To that end, a quantification of the impact of high field on machine cost was carried out. The methodology applied is based on the use of unit costs,

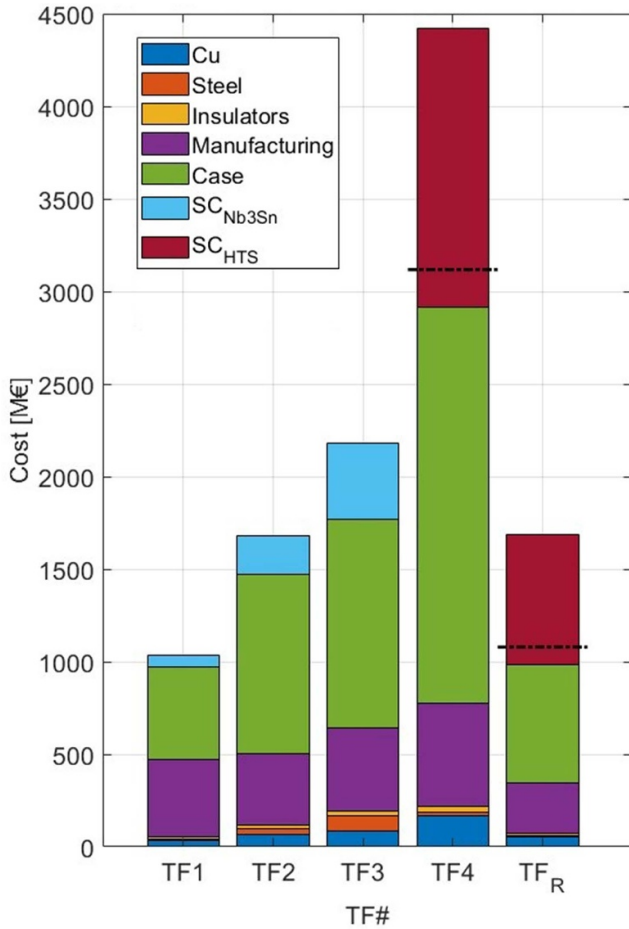


Figure 8. Total TF coil cost and breakdown for each of the machine configurations shown in figures 5 and 6 (variable aspect ratio and power). All cases (LTS and HTS) assume standard windings without radial plates. The black dashed horizontal lines on TF4 and TF_{4R} represent the total cost in the assumption unit cost of HTS is the same as that of Nb₃Sn.

so that it is possible to update these estimates over time in case of escalation or more refined estimates for fabrication costs. Therefore, the cost estimates for unit material costs (e.g. superconductor, steel, etc) are in €/kg, and fabrication costs are in the appropriate unit (e.g. €/m). For the TF coil cost analyses detailed here, these unit costs are applied to the different configurations as the magnetic field is varied, and the winding pack and structures are designed accordingly.

These ‘bottoms-up’ cost estimates should be considered as accurate in relative terms to one another, but as they do not include other commercial or contractual considerations, they may not be accurate in absolute terms without further benchmarking.

The cost analysis is a function of the level of detail with which the system is divided. The breakdown of sub-components for this study is as follows:

1. Superconducting material (Nb₃Sn or HTS)
2. Stabilizer material (copper)
3. Steel for the CICC's jacket
4. Insulating material

5. Manufacturing: cabling, jacketing, winding, and heat treatment (for LTS coils only)
6. TF coil case (including materials and manufacturing)

The conclusions of the cost estimates are shown in figure 8, where the total cost is given for each of the five TF coil configurations described in section 4 above. All cases considered in figure 8 (LTS or HTS) do not contain radial plates, all designs are for standard windings. Also shown is the breakdown by major component in each case. As expected, the overall TF coil cost increases with magnetic field, and two effects in particular are notable. The cost of materials and manufacturing for the TF coil structures plays a major role and becomes dominant as the magnetic field increases (and this is to be expected). Given the current unit costs for HTS, the superconductor component of overall cost also becomes dominant at high field. In this study, and based on current market prices, it is assumed that the unit cost of HTS wire (€/kg) is 7 times higher than that of LTS. This factor is not necessarily a reflection of raw material cost, but rather maturity level, as HTS is not yet produced at the same volumes as LTS. The price ratio of HTS to LTS is likely to drop as production volumes increase. In figure 8 this is indicated by the black dashed horizontal line representing the total cost of an insulated HTS coil in the assumption unit costs of superconductor (LTS or HTS) are the same. The cost of coil manufacturing in the case of HTS does not include a heat treatment step (~4% saving on total cost). Notice however, that even if HTS cost were to drop to equal the costs of LTS, or even lower, the overall TF coil cost significantly increases with magnetic field as the structures become heavier and harder to fabricate.

6. TF coil structural material selection and fabrication considerations

In addition to electromagnetic, structural, or cost considerations in the design of the TF coils, aspects such as manufacturability and schedule are also determinant, in particular, development time for the introduction of new materials, technologies, or manufacturing processes. This is relevant in light of the results shown in section 4.3.

Developing and qualifying new and stronger structural materials is a long and arduous road as demonstrated by ITER. As stated in [17], magnets of large reactor scale need large quantities of such steels, and novel steels (often with unusual constituents such as Nb or Mn) come with novel forging and welding problems to which industrial suppliers are unable to offer solutions. Multiple high-strength steel developments for ITER, launched in the 1990s, were all discarded by 2010, with one exception (used in the inner leg of the ITER TF coil cases) and, even here, the original targets have been much relaxed. An example of the problems that can occur with novel (and not fully investigated) steels is discussed in [23].

Another notable example was the development of a nickel based super alloy, called Incoloy as a jacket material for Nb₃Sn. Although thermal and mechanical characteristics of Incoloy were deemed promising, it was found to be highly sensitive to oxygen embrittlement [24]. Therefore, although

Incoloy was used successfully in the ITER model coils, catastrophic failure in operation arising from the problems of oxygen control in large-scale industrial production presented an unacceptable risk to the project. As a result, Incoloy was finally eliminated as an option from the magnet design in 2003.

In addition to materials development time, there is a significant lead time for the development of manufacturing processes and tooling.

Within the architecture of wedged structures, there is a practical limit to the thickness of the TF coil nose given by maximum size of forgings. Larger TF coil structures also make manufacturability impractical as weld deformation control of large/thick sections becomes extremely challenging. Lead time for the procurement of materials and forgings can be a major portion of overall construction schedule for a fusion power plant. The need to prepare welding mock-ups can significantly add to any structure fabrication schedule.

An industrial study for DEMO-size fusion power plant machines reached the conclusions that not only cost and schedule of TF coil structures are major drivers, but also that it is the structures that dominate the cost of the TF coils (as also shown here, see section 5). These conclusions are also supported by the ITER experience, where even using three suppliers in parallel, the rate of production of TF coil structures set the limit on TF coil manufacturing and delivery rate. Furthermore, it was not just an issue of production schedule, but the TF coil structures were also responsible for multiple delays and technical challenges related to the production of very heavy components while maintaining tight dimensional tolerances. Also based on ITER experience [25, 26], the time needed to produce all the TF coil structures (even with three lines in parallel), and the time needed to procure materials, produce forgings, complete welding mock-ups, and prepare the tooling are about equal. Meaning that the schedule to produce TF coils in a tokamak is greatly determined by the structures and, depending on overall size/mass, spans over a decade from start to finish.

Therefore, any optimization of machine configuration should take these factors into account and drive the design towards lighter structures, which in turn drives a shift towards lower magnetic fields, not higher.

7. Fusion-relevant HTS development

The fact the study concludes there is no advantage (technical or cost) to push fusion machines towards higher fields does not mean HTS materials do not have a major role to play in future fusion development. The other meaningful property of HTS comes into play, namely its ability to operate at higher temperature. This property can be used to design magnets with much higher operating margin, which in turn allows to make the cooling simpler (conduction-cooled magnets, or magnets in which the cooling is not part of the conductor). Separation of function in the conductor (current-carrying and cooling), could not only lead to simplification of magnet fabrication, but also major de-risking in terms of high-voltage operation or Paschen discharges. Cooling of the winding pack could be

done externally, and the hydraulic circuit does not necessarily need to be at high-voltage. Conduction-cooling of the winding pack allows the pipes to be placed outside the ground plane, and electrical breaks in the hydraulic circuit can be obviated, eliminating both electrical and leak risks. HTS are the enabling technology for ‘dry magnets’. Therefore, extraction of conductor and wires at the terminals, although not a trivial problem, becomes significantly easier without having to accommodate the coolant, and voltage tracking or Paschen discharge risks in the terminal region are reduced.

Despite the obvious advantages of HTS in simplifying magnet winding, an area still in need of development is quench protection. It is well known in the design of superconducting magnets that there is a trade-off between magnet stability and quench protection. In a magnet with very low stability margin, a quench, once initiated, will tend to propagate rapidly, meaning that is relatively easy to detect early, and protect the magnet accordingly. The converse is also true, in a very stable magnet, a quench will not propagate very fast, making it hard to detect and protect against (as reaction time is greatly diminished). In fact, in highly stable magnets, the existence of persistent travelling normal zones is also a possibility. In a HTS magnet operating at higher temperature, the winding pack heat capacity is at least an order of magnitude higher than at 4 K, meaning the condition of a highly stable coil is difficult to protect against quench. This challenge from operating at high temperature is well recognized since shortly after the discovery of HTS. Even though much work has gone into developing means to detect and protect HTS magnets during quench, with multiple ideas proposed including use of fibre optics [27–29], ultrasonics [30], or NI coils [31–33], it remains an area of active research and none of these novel approaches has reached sufficient maturity to be deployed in fusion-scale magnets. The challenge of quench protection for HTS coils obviously grows with the size (stored energy) of the coil, especially if high current densities are sought. To date, despite good operational experience with HTS magnets, no coil of fusion-relevant size has been shown to be able to survive a quench event. It should be stressed that from ITER experience as well as from other large-scale projects, that adoption of new and untested technology promising leaps in performance, comes with very long development cycles. It is not unusual for such development and qualification cycles to be measured decades before a technology can reach sufficient maturity for implementation into a power plant. Therefore, the fundamental challenge for the future of HTS application in large-scale fusion magnets, is not improvements to the material, but rather development and qualification of quench protection schemes, as has been recognized for many years now.

The development of conduction-cooled magnet concepts, quench protection schemes applicable at relevant scale, and characterization of HTS conductor neutron radiation damage should be the cornerstones of any fusion-centric HTS magnet R&D programme. The culmination of such a programme would be the design, fabrication, and test of an HTS model coil with size and characteristics that demonstrate and de-risk the technology prior to deployment on a power plant. EUROfusion is presently working on the development and coordination

of such HTS development programme to be carried out by European fusion institutions in cooperation with industry.

8. Conclusions

This paper analysed the scalability of tokamaks when increasing the plasma (and coil) magnetic field in an attempt to reduce size via higher fusion power density. Higher field windings generate higher forces in the mechanical structures in and around the plasma and in particular in the TF coil themselves. The stresses in the inboard leg of the TF coil casing quickly reach the maximum allowable stress for a given geometry, effectively limiting any further size reduction brought by increasing the field. The study detailed within this paper shows that, for large power-plant size tokamaks, and under the assumption of wedged TF coil structures, increasing the field does not lead to a reduction in machine size. Once structural, power exhaust, cost, and other practical considerations are included, simply increasing the magnetic field does not lead to smaller and cheaper machines. Employing steels with a much higher yield strength reduces the size of the machine, but does not alter the scalability behaviour, meaning that increasing magnetic field still does not lead to size reductions beyond a certain point. This is intrinsic to the structural concept, not the material properties. More advanced structural support concepts have been explored and it was concluded that most of the solutions considered are either unfeasible or do not provide sufficient size reduction when trying to increase field. The fact remains that if machine size reductions are being pursued via HTS materials and high field operation, structural concepts with different scalability behaviour need to be developed, the conventional approach of TF coil wedging will not achieve it.

This is not to say HTS do not offer other advantages for the simplification and de-risking of fusion magnets. These include the potential simplification of the magnet cooling scheme thanks to increased temperature margin (indirect conduction cooling), which in turn can greatly simplify coil construction and minimize high-voltage risks at the terminals by decoupling coolant and current-carrying functions of the conductor. A development programme is proposed to bring HTS to the level of maturity needed for adoption in fusion-scale magnets. EUROfusion is the process of articulating and implementing such development and qualification programme.

Acknowledgments

The authors thank Michel Huguet, Pietro Barabaschi, and Luca Bottura for useful discussions and insights.

This work has been carried out within the framework of the EUROfusion Consortium, funded by the European Union via the Euratom Research and Training Programme (Grant Agreement No. 101052200—EUROfusion). Views and opinions expressed are however those of the author(s) only and do not necessarily reflect those of the European Union or the European Commission. Neither the European Union nor the European Commission can be held responsible for them.

ORCID iD

M. Lungaroni  <https://orcid.org/0000-0002-1500-363X>

References

- [1] Thome R.J. and Tarrh J.M. 1982 *MHD and Fusion Magnets: Field and Force Design Concepts* (Wiley) pp 243–50
- [2] Huguet M. 1997 The ITER magnet system *Fusion Eng. Des.* **36** 23–32
- [3] Mitchell N., Devred A., Libeyre P., Lim B. and Savary F. 2012 The ITER magnets: design and construction status *IEEE Trans. Appl. Supercond.* **22** 2174560
- [4] Creely A.J. et al 2020 Overview of the SPARC tokamak, published online by Cambridge University Press *J. Plasma Phys.* **86** 865860502
- [5] Greenwald M. 2020 Status of the SPARC physics basis, published online by Cambridge University Press *J. Plasma Phys.* **86** 861860501
- [6] Corato V. et al 2022 The DEMO magnet system—status and future challenges *Fusion Eng. Des.* **174** 112971
- [7] Bachmann C., Siccino M., Albino M., Chiappa A., Falcitelli G., Federici G., Giannini L. and Luongo C. 2023 Influence of a high magnetic field to the design of EU DEMO *Fusion Eng. Des.* **197** 114050
- [8] Eich T., Sieglin B., Scarabosio A., Fundamenski W., Goldston R.J. and Herrmann A. 2011 Inter-ELM power decay length for JET and ASDEX upgrade: measurement and comparison with heuristic drift-based model *Phys. Rev. Lett.* **107** 215001
- [9] Eich T. et al 2013 Scaling of the tokamak near the scrape-off layer H-mode power width and implications for ITER *Nucl. Fusion* **53** 093031
- [10] Martin Y.R. and Takizuka T. (The ITPA CDBM H-mode Threshold Database Working Group) 2008 Power requirement for accessing the H-mode in ITER *J. Phys.: Conf. Ser.* **123** 012033
- [11] Wenninger R. et al 2017 The DEMO wall load challenge *Nucl. Fusion* **57** 046002
- [12] Siccino M., Federici G., Kembleton R., Lux H., Maviglia F. and Morris J. 2019 Figure of merit for divertor protection in the preliminary design of the EU-DEMO reactor *Nucl. Fusion* **59** 106026
- [13] Whyte D. et al 2010 I-mode: an H-mode energy confinement regime with L-mode particle transport in Alcator C-Mod *Nucl. Fusion* **50** 105005
- [14] Hubbard A.E. et al 2017 Physics and performance of the I-mode regime over an expanded operating space on Alcator C-Mod *Nucl. Fusion* **57** 126039
- [15] Austin M.E. et al 2019 Achievement of reactor-relevant performance in negative triangularity shape in the DIII-D tokamak *Phys. Rev. Lett.* **122** 115001
- [16] Kikuchi M. et al 2019 L-mode-edge negative triangularity tokamak reactor *Nucl. Fusion* **59** 056017
- [17] Campbell D.J. et al 2019 Innovations in technology and science R&D for ITER *J. Fus. Energy* **38** 11–71
- [18] Fable E., Angioni C., Siccino M. and Zohm H. 2018 Plasma physics for fusion reactor system codes: framework and model code *Fusion Eng. Des.* **130** 131–6
- [19] Sarasola X., Bruzzone P., Sedlak K., Corato V., Giannini L., Bachmann C., Luongo C. and Siccino M. 2023 Parametric studies of the EU DEMO central solenoid *IEEE Trans. Appl. Supercond.* **33** 4201205
- [20] Giannini L. et al 2023 The magnet design explorer algorithm (MADE) for LTS hybrid, or HTS toroidal and poloidal systems of a tokamak with a view to DEMO *Fusion Eng. Des.* **193** 113659

- [21] Federici G. *et al* 2019 Overview of the DEMO staged design approach in Europe *Nucl. Fusion* **59** 066013
- [22] Bachmann C. *et al* 2017 Overview of DEMO design integration challenges and their impact on component design concepts *Fusion Eng. Des.* **136** 87–95
- [23] Nakajima H., Yoshida K. and Shimamoto S. 1990 Development of new cryogenic steels for the superconducting magnets of the fusion experimental reactor *ISIJ Int.* **30** 567–78
- [24] Libeyre P. *et al* 2001 Risks and benefits of Incoloy 908 *Fusion Eng. Des.* **58-59** 129–34
- [25] Sakurai T., Iguchi M., Nakahira M., Inagaki T., Matsui K. and Koizumi N. 2016 Development of manufacturing technology for ITER TF coil structure *Fusion Eng. Des.* **109-11** 1592–7
- [26] Nakahira M. *et al* 2019 Completion of the first ITER TF coil structure *Nucl. Fusion* **59** 086039
- [27] van Oort J.M., Scanlan R.M. and ten Kate H.H.J. 1995 A fiber-optic strain measurement and quench localization system for use in superconducting accelerator dipole magnets *IEEE Trans. Appl. Supercond.* **5** 882–5
- [28] Liu Y., Fisser M., Fang J., Jiang Z., Mataira R. and Badcock R.A. 2019 Feasibility study of fiber Bragg grating sensor for quench detection of high temperature superconductors *IEEE Trans. Appl. Supercond.* **29** 9001606
- [29] Huang X., Davies M., Moseley D.A., Gonzales J.T., Weijers H.W. and Badcock R.A. 2022 Sensitive fiber optic sensor for rapid hot-spot detection at cryogenic temperatures *IEEE Sens. J.* **22** 11775
- [30] Marchevsky M., Prestemon S., Lobkis O., Roth R., van der Laan D.C. and Weiss J.D. 2022 Ultrasonic waveguides for quench detection in HTS magnets *IEEE Trans. Appl. Supercond.* **32** 4701705
- [31] Hahn S., Park D.K., Bascunan J. and Iwasa Y. 2011 HTS pancake coils without turn-to-turn insulation *IEEE Trans. Appl. Supercond.* **21** 1592–5
- [32] Wang Y., Chan W.K. and Schwartz J. 2016 Self-protection mechanisms in no-insulation (RE)Ba₂Cu₃O_x high temperature superconductor pancake coils *Supercond. Sci. Technol.* **29** 045007
- [33] Dong F., Park D., Kim J., Bascunan J. and Iwasa Y. 2023 Sudden-discharging quench dynamics in a no-insulation superconducting coil *IEEE Trans. Appl. Supercond.* **33** 4600105